B-cell receptor triggers drug sensitivity of primary CLL cells by controlling glucosylation of ceramides

Janine Schwamb,[1-3] Valeska Feldhaus,[1-3] Michael Baumann,[1-3] Michaela Patz,[1-3] Susanne Brodesser,[3,4] Reinhild Brinker,[1-3] Julia Claasen,[1-3] Christian P. Pallasch,[1-3] Michael Hallek,[1-3] *Clemens-Martin Wendtner,[1-3,5] and *Lukas P. Frenzel[1-3]

[1]Department I of Internal Medicine, [2]Center of Integrated Oncology, [3]Cologne Excellence Cluster on Cellular Stress Responses in Aging-Associated Diseases, and [4]Institute for Medical Microbiology, Immunology and Hygiene, University of Cologne, Cologne, Germany; and [5]Department I of Internal Medicine, Klinikum Schwabing, Munich, Germany

Survival of chronic lymphocytic leukemia (CLL) cells is triggered by several stimuli, such as the B-cell receptor (BCR), CD40 ligand (CD40L), or interleukin-4 (IL-4). We identified that these stimuli regulate apoptosis resistance by modulating sphingolipid metabolism. Applying liquid chromatography electrospray ionization tandem mass spectrometry, we revealed a significant decrease of proapoptotic ceramide in BCR/IL-4/CD40L–stimulated primary CLL cells compared with untreated controls. Antiapoptotic glucosylceramide levels were significantly increased after BCR cross-linking. We identified BCR engagement to catalyze the crucial modification of ceramide to glucosylceramide via UDP-glucose ceramide glucosyltransferase (UGCG). Besides specific UGCG inhibitors, our data demonstrate that IgM-mediated UGCG expression was inhibited by the novel and highly effective PI3Kδ and BTK inhibitors CAL-101 and PCI-32765, which reverted IgM-induced resistance toward apoptosis of CLL cells. Sphingolipids were recently shown to be crucial for mediation of apoptosis via mitochondria. Our data reveal ABT-737, a mitochondria-targeting drug, as interesting candidate partner for PI3Kδ and BTK inhibition, resulting in synergistic apoptosis, even under protection by the BCR. In summary, we identified the mode of action of novel kinase inhibitors CAL-101 and PCI-32765 by controlling the UGCG-mediated ceramide/glucosylceramide equilibrium as a downstream molecular switch of BCR signaling, also providing novel targeted treatment options beyond current chemotherapy-based regimens. (*Blood*. 2012;120(19):3978-3985)

Introduction

Despite recent advances in the treatment of chronic lymphocytic leukemia (CLL) by use of modern chemoimmunotherapies,[1,2] the disease remains incurable for most patients with the exception of those who have the option of an allogeneic transplantation.[3] Moreover, most chemotherapeutic regimens require a certain physical fitness of the patient. Because CLL is a disease of the elderly, there is a need for novel therapeutic concepts, which are able to disrupt resistance to cytostatic drugs. Chemoresistance is thought to be partially the result of malignant cell clones that find a niche within the microenvironment. Resistance might be mediated at least by 3 major stimuli: (1) by engagement of the B-cell receptor (BCR), (2) by CD40 ligand (CD40L)-CD40 interaction, and (3) by stimulation via interleukin-4 (IL-4).[4] Those signals lead via downstream pathways to reduced susceptibility of CLL cells toward chemotherapy within the microenvironment. To some extent, these stimuli share common pathways to mediate survival.[5] As a consequence, the balance between proapoptotic and antiapoptotic signals is disrupted toward pro-survival signals. BCR signaling has been identified as the central and determining factor in CLL. Therefore, novel compounds, which target this pathway, have been developed: CAL-101 as PI3Kδ inhibitor and PCI-32765 as inhibitor of Bruton tyrosine kinase (BTK).

Recent data from first trials using CAL-101 and PCI-32765 indicate that inhibition of the BCR pathway leads to the redistribution of CLL cells from local compartments (spleen, liver, lymph nodes) resulting in peripheral lymphocytosis.[6-10] However, the precise mode of action of these drugs in vivo remains unclear.

We and other groups have found recently that BCR signaling causes a deregulation of lipid metabolism-associated genes in CLL cells.[11,12] For sphingolipid metabolism, the metabolites being responsible for survival and chemoresistance in CLL cells are partially known.[13] However, the regulation of the sphingolipid equilibrium is poorly understood.

Sphingolipids act as effector molecules in lipid metabolism involving numerous components and derivates, such as ceramide and its counterpart glucosylceramide.[14,15] The structure of sphingolipids consists of a sphingoid long chain base, which is connected to a fatty acid chain of varying length via amino bond.[16] Beyond that, it could be shown that the length of fatty acid chain influences diverse functions of sphingolipids.[17,18] C16 displays the most common chain length of ceramides in non-neuronal tissues and is supposed to be the leading ceramide during apoptosis.[17] However, for primary malignant B cells and especially CLL cells, the composition of ceramides is unknown. Ceramide can be synthesized by de novo pathway out of serine and palmitoyl-CoA or by several other mechanisms (eg, hydrolysis of sphingomyelin). Importantly, ceramide serves as substrate for UDP-glucose ceramide glucosyltransferase (UGCG) resulting in glucosylceramide

Submitted May 21, 2012; accepted August 5, 2012. Prepublished online as *Blood* First Edition paper, August 27, 2012; DOI 10.1182/blood-2012-05-431783.

*C.-M.W. and L.P.F. contributed equally to this study.

There is an Inside *Blood* commentary on this article in this issue.

The online version of this article contains a data supplement.

The publication costs of this article were defrayed in part by page charge payment. Therefore, and solely to indicate this fact, this article is hereby marked "advertisement" in accordance with 18 USC section 1734.

as product. Interestingly, ceramide and glucosylceramide function in an antagonistic fashion. Whereas elevated levels of unmodified ceramide contribute to apoptosis and growth inhibition,[14,15] glucosylceramide particularly mediates proliferative mechanisms, including malignant transformation and resistance to apoptosis.[13,14]

Here we report the impact of pro-survival signals, such as engagement of the BCR as well as stimulation by CD40L or IL-4 on sphingolipid metabolism of CLL cells and its impact on resistance toward apoptosis.

Methods

Patient samples

After informed consent was given, blood was obtained from CLL patients. Fresh CLL samples were enriched by applying B-RosetteSep (StemCell Technologies) and Ficoll-Hypaque (Seromed) density gradient purification, resulting in purity > 95% of $CD19^+/CD5^+$ CLL cells. Isolated cells were cultured as described in "Treatment of cells." This study was approved by the ethics committee of the University of Cologne; blood samples were given with informed consent according to the Helsinki protocol. Characteristics of patients' samples are given in supplemental Table 1 (available on the *Blood* Web site; see the Supplemental Materials link at the top of the online article).

Treatment of cells

Freshly isolated cells were resuspended in IMDM (Invitrogen) supplemented with 10% heat-inactivated FCS, 2mM L-glutamine, 100 U/mL penicillin, and 100 μg/mL streptomycin and treated with either 25 μL/mL anti–IgM-polyacrylamide Immunobead reagent (Irvine Scientific) or with 25 ng/mL IL-4 (PeproTech). CD40L stimulation of CLL cells was performed by cultivation on irradiated human CD40L-expressing NIH3T3 fibroblasts as feeder layer cocultivation system.[19] Native cells served as control sample. Native and treated cells were then incubated for 3 or 24 hours, depending on the following experimental design, at 37°C in 5% CO_2 humidified atmosphere.

Lipid analysis

Sphingolipid levels in CLL and healthy donor B-cell controls were determined by liquid chromatography coupled to electrospray ionization tandem mass spectrometry (LC-ESI-MS/MS) using a procedure previously described[20] with several modifications: $\sim 3 \times 10^7$ cells were homogenized in 300 μL of water using the Precellys 24 Homogenisator (Peqlab). The protein content of the homogenate was routinely determined using bicinchoninic acid. To 100 μL of homogenate 750 μL of methanol/chloroform 2:1 (volume/volume) and internal standards (100 pmol ceramide 17:0, 500 pmol sphingomyelin 17:0, both Matreya; 122 pmol glucosylceramide 12:0, Avanti Polar Lipids) were added. Lipids were extracted overnight at 48°C. Interfering glycerolipids were degraded by alkaline hydrolysis adding 75 μL of 1M potassium hydroxide in methanol and incubating for 2 hours at 37°C. After neutralization with glacial acetic acid, the lipid extract were purified using a modification of the Bligh-Dyer procedure as previously described.[21] Dried lipid extracts were resolved in 600 μL of mobile phase solvent A (see below). LC-MS/MS analysis was performed using a normal phase Nucleosil NH_2 column (50 mm × 2 mm ID, 3 μm particle size, 120 Å pore size, Macherey-Nagel) with detection using a 4000 QTrap mass spectrometer (AB SCIEX). The LC (1200 Series Binary LC System, Agilent) was operated at a flow rate of 0.75 mL/min with a mobile phase of acetonitrile/methanol/acetic acid 97:2:1 (volume/volume/volume) with 5mM ammonium acetate (solvent A) and methanol/acetic acid 99:1 (volume/volume/volume) with 5mM ammonium acetate (solvent B). After injection of 20 μL of sample, 100% A was applied for 0.5 minutes, then linearly changed to 90% A/10% B in 0.2 minutes and held for 0.5 minutes, then linearly changed to 82% A/18% B in 0.4 minutes and held for 0.6 minutes, followed by a 0.4-minute linear gradient to 100% B, which was maintained for 1.9 minutes and finally restored to 100% A by a 0.4-minute linear gradient and held for 1.6 minutes to reequilibrate the column. Sphingolipid species were monitored in the positive ion mode with their specific multiple reaction monitoring transitions.[20] The instrument settings for nebulizer gas (gas 1), turbogas (gas 2), curtain gas, and collision gas were 50 psi, 55 psi, 20 psi, and medium, respectively. The interface heater was on, the Turbo V ESI source temperature was 400°C, and the ionspray voltage was 5.5 kV. For all multiple reaction monitoring transitions, the values for declustering potential, entrance potential, and cell exit potential were 80, 10, and 14 V, respectively. The collision energies ranged from 35 to 55 V. Quantification was achieved by correlating the peak areas relating to the endogenous lipid species with those of the internal standards.[20]

RNA isolation and cDNA synthesis

RNA isolation was performed by lysis of cells with TRIZOL reagent (Invitrogen) at room temperature. For extraction and phase separation, chloroform was added followed by centrifugation. RNA in the aqueous phase was isolated and precipitated with isopropanol. After centrifugation for 30 minutes at 12 000*g*, RNA was washed twice with 70%-80% ethanol, dried and dissolved in RNAse-free water, and finally incubated for 5-10 minutes at 55°C. cDNA synthesis for subsequent PCR was performed using cDNA-synthesis Kit (Roche Diagnostics).

Quantitative RT-PCR

Quantification of UGCG mRNA was performed by LightCycler Taqman Master (Roche Diagnostics). Universal probe No. 4 (Roche Diagnostics) with forward primer 5′-ATTCAATTTCTCAGTTTCAATCCA-3′ and reverse primer 3′-ATTCTGAAATTGGCTCACAAATTA-5′ was used for UGCG amplification. β-actin was applied as housekeeping gene standard by Universal probe no. 64 (Roche Diagnostics) with forward primer 5′-CCAACCGCGAGAAGATGA-3′ and reverse primer 3′-CCAGAGGCGTACAGGGATAG-5′. All experiments were performed in replicates, and crossing points were determined by second derivative maximum method. Relative quantification analysis was performed by Exxor3 software package (Roche Diagnostics).

Treatment of primary CLL cells with N-(n-Butyl)deoxygalactonojirimycin (OGB-1), N-(n-Nonyl)deoxygalactonojirimycin (OGB-2), ABT-737, CAL-101, and PCI-32765

Primary CLL cells were isolated as previously described. A total of 4×10^6 cells were used for treatment and subsequent flow cytometry analysis. Cells were treated with OGB-1 and OGB-2 (Santa Cruz Biotechnology) in a concentration of 1000μM and 20μM, respectively. A total of 25 μL/mL anti–IgM-polyacrylamid Immunobead reagent (Irvine Scientific) was added 30 minutes after OGB addition. After incubation for 24 hours at 37°C in 5% CO_2 humidified atmosphere, CLL cells were treated with ABT-737 (Selleck Chemicals) in a concentration of 4nM. After another incubation period of 24 hours, cells were prepared for flow cytometric analysis. Samples for mass spectrometry were treated the same.

Treatment with CAL-101 and PCI-32765 was performed similarly. A total of 1×10^7 primary CLL cells per well were treated with 0.5μM CAL-101 (Selleck Chemicals) or 1μM PCI-32765 (Selleck Chemicals), respectively. After 30 minutes 20 μL/mL anti–IgM-polyacrylamide Immunobead reagent (Irvine Scientific) was applied. After another time period of 30 minutes, ABT-737 (Selleck Chemicals) was added in a concentration of 4nM. After 3 hours, samples were collected for quantitative RT-PCR. After a total incubation time of 24 hours, samples were prepared for flow cytometric analysis.

Flow cytometry

Apoptosis was determined by flow cytometry using annexin V-FITC/7-amino-actinomycin D staining (BD Biosciences PharMingen). Measurement was carried out by FACSCanto flow cytometry (BD Biosciences PharMingen).

Statistics

Statistical analysis was performed using Excel (Microsoft) and GraphPad Prism Version 4.0c. In particular, paired 2-tailed *t* test, unpaired 2-tailed *t* test, and Wilcoxon signed-rank test were applied.

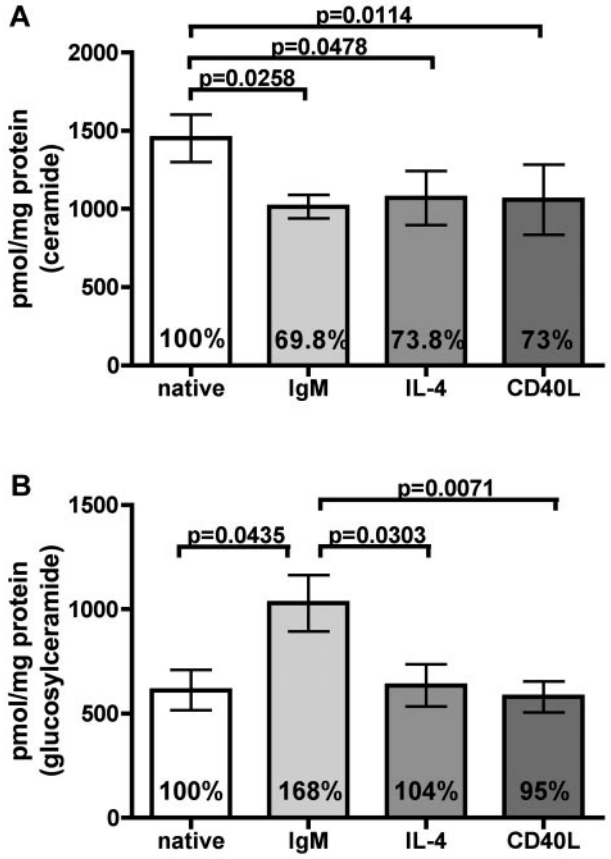

Figure 1. BCR-mediated chemoresistance differs from CD40L and IL-4 by regulating ceramides and glucosylceramides levels. LC-ESI-MS/MS was applied to determine sphingolipid levels in CLL cells from 8 patients. (A) After stimulation with anti-IgM immunobeads, IL-4, and CD40L for 24 hours, a reduction of apoptotic ceramide levels could be observed (IgM, $P = .0258$; IL-4, $P = .0478$; CD40L, $P = .0114$). (B) Pro-survival glucosylceramide was exclusively increased after BCR engagement ($P = .0435$). Data are mean ± SEM of the sums of all analyzed fatty acyl subspecies per analyzed sample of 8 independent experiments. Statistics are calculated by paired *t* test.

Results

Distinct ceramide/glucosylceramide equilibrium mediated by BCR, CD40L, and IL-4

It is well known that stimulation of the BCR, by CD40L or IL-4, leads to survival and drug resistance of CLL cells.[4] We were interested whether engagement of these receptors has any influence on the sphingolipid composition of CLL cells. Whereas high amounts of ceramides are associated with proapoptotic features,[14,15] elevated glucosylceramide levels promote a pro-survival status in malignant cells.[13] Because we hypothesized that these stimuli themselves might regulate the sphingolipid "rheostat," we performed LC-ESI-MS/MS of CLL cells of 8 persons. Before analysis, cells were treated with anti-IgM immunobeads for 24 hours, whereas untreated samples served as controls. As additional pro-survival stimuli, CLL cells were further incubated with IL-4 and on CD40L expressing feeder cells (CD40L). Ceramide levels were significantly reduced after treatment with anti-IgM, IL-4, and CD40L (IgM, $P = .0258$; IL-4, $P = .0478$; CD40L, $P = .0114$), indicating that these stimuli are involved in sphingolipid-mediated antiapoptotic pathways (Figure 1A). In contrast, glucosylceramide levels were exclusively and significantly increased after BCR stimulation ($P = .0435$) independently of the IGHV mutational status and cytogenetics (date not shown), whereas other stimuli had no influence on its regulation (Figure 1B). These stimuli had no effect on the amount of sphingomyelins (supplemental Figure 1). In conclusion, the ceramide/glucosylceramide equilibrium shows a prerequisite pattern for BCR signaling involving both antagonistic mediators being altered from a pro-apoptosis toward a pro-survival pattern.

C16:0 and C24:1 sphingolipids are predominantly expressed and controlled by BCR in CLL cells

We were interested to further specify molecular characteristics of ceramides involved in apoptosis regulation. Therefore, we analyzed sphingolipid subspecies acylated by different fatty acids in native and IgM stimulated CLL cells by mass spectrometry to identify the relevant chain lengths of sphingolipids in CLL cells. Our mass spectrometric analysis reveals C16:0 and C24:1 as the predominant fatty acyl chains in CLL cells (Figure 2). BCR engagement significantly reduces ceramide levels of different fatty acyl chain lengths, especially of the most highly abundant C16:0 and C24:1 compared with untreated CLL cells (C16:0, $P < .0001$; C24:1, $P = .0010$; Figure 2A). Moreover, BCR stimulation leads to a significant increase of glucosylceramide levels compared with untreated cells (C16:0, $P = .0004$; C24:1, $P = .0012$; Figure 2B). In total, BCR-associated survival is accompanied by decreased ceramide and increased glucosylceramide levels.

Besides the stress- or receptor-induced sphingomyelin cycle, sphingomyelin is biosynthesized out of ceramide by de novo pathway. In contrast, it can be cleaved into ceramide and subsequently metabolized into fatty acids and sphingoid. In this context, we wanted to investigate whether changes in ceramide levels result from metabolism into sphingomyelins or vice versa (supplemental Figure 2). Therefore, we determined sphingomyelin levels by mass spectrometry. Importantly, comparing sphingomyelin amounts in CLL cells, no relevant differential regulation between native and IgM-stimulated cells could be observed, demonstrating that sphingomyelin is not substantially involved in regulation of ceramide composition (Figure 2C). To directly compare and relate ceramide and glucosylceramide levels in CLL, we generated a ceramide/glucosylceramide ratio out of the former mass spectrometric expression data (Figure 2D; supplemental Figure 3). Throughout all fatty acyl chains, native CLL samples display a higher ratio, which represents a higher ceramide and lower glucosylceramide level. In contrast, higher glucosylceramide and decreased ceramide levels were observed in IgM-treated samples with a concomitant lower ratio, suggesting novel components of pro-survival features of IgM stimulated cells (Figure 2D). These results indicate that a shift of the ceramide/glucosylceramide ratio toward a apoptosis-resistant phenotype might be regulated by an enzymatic step between ceramides and glucosylceramides and is not related to sphingomyelin metabolism.

BCR controls chemoresistance of CLL cells via UGCG

Thus, we investigated whether the key enzyme UGCG catalyzes the glucosylation step in glucosphingolipid biosynthesis, resulting in increased glucosylceramide after BCR stimulus. To evaluate whether UGCG expression changes after BCR stimulation, we performed quantitative RT-PCR of CLL samples (n = 19). After BCR engagement, independently of IGHV mutational status, a significant increase in UGCG expression in CLL cells could be shown ($P = .0001$; Figure 3), whereas CD40L had no influence on UGCG regulation (supplemental Figure 4). As a consequence, we

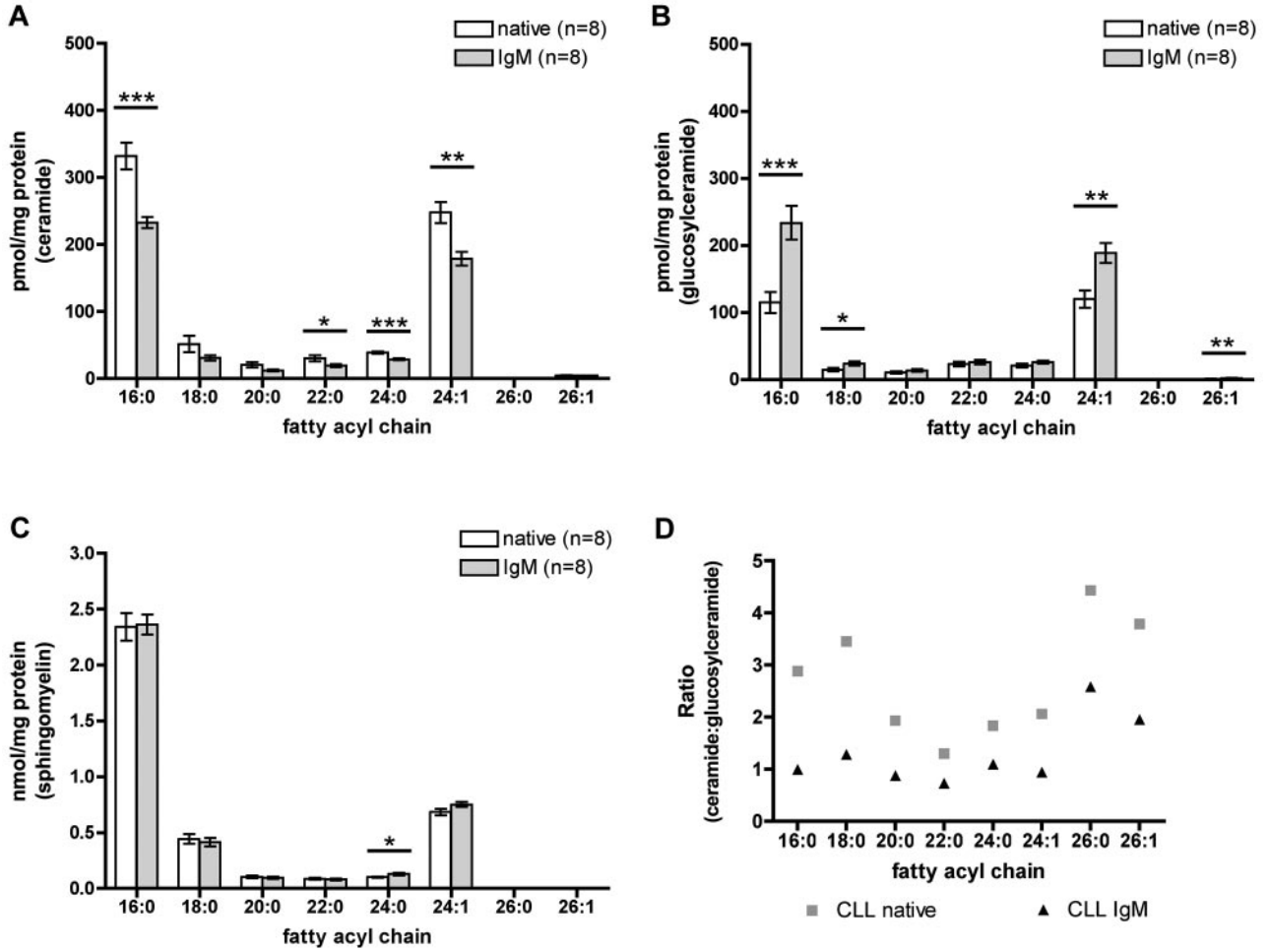

Figure 2. Identification of major sphingolipid chain lengths involved in chemoresistance, which are regulated by BCR in primary CLL cells. LC-ESI-MS/MS with differentiation between distinct fatty acyl subspecies of sphingolipids after BCR stimulation for 24 hours was applied (n = 8). (A) Ceramide levels were significantly reduced after BCR engagement compared with native controls, especially of the most highly abundant C16:0 and C24:1 (C16:0, $P < .0001$; C24:1, $P = .0010$). (B) IgM stimulation caused a significant increase in glucosylceramide (C16:0, $P = .0004$; C24:1, $P = .0012$). (C) Sphingomyelin levels showed no differences between native and IgM-stimulated samples. (D) Ceramide/glucosylceramide ratio based on mass spectrometric data: A higher quotient of the ratio reveals an increase of ceramide, whereas a lower ratio indicates higher glucosylceramide levels. BCR cross-linking reverted the ratio toward pro-survival glucosylceramide associated with a lower ratio. Results of LC-ESI-MS/MS are expressed as mean ± SEM of 8 independent experiments. Statistics are calculated by unpaired *t* test.

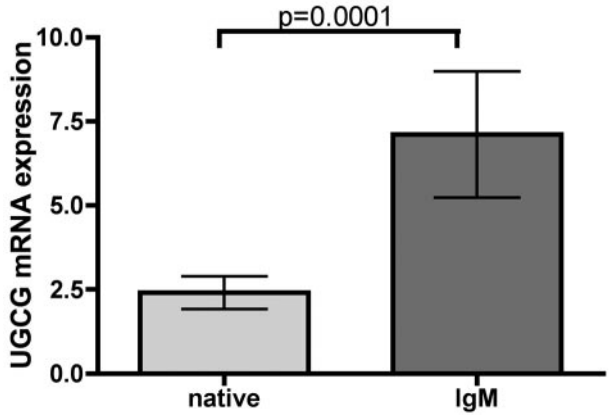

Figure 3. BCR controls chemoresistance of CLL cells via UGCG. Analysis of UGCG enzyme expression was carried out via quantitative RT-PCR. A significant induction of UGCG enzyme expression could be induced after BCR stimulation for 3 hours (n = 19, $P = .0001$). Data are mean ± SEM of 19 independent experiments. Statistics are calculated by Wilcoxon signed-rank test.

hypothesized that specific inhibition of UGCG might be able to reverse the ceramide/glucosylceramide ratio toward ceramide after IgM stimulation and thereby testing whether UGCG is crucial for glucosylceramide development after IgM stimulation. Second, we were interested to investigate whether reversion of the ceramide/glucosylceramide ratio might sensitize CLL cells toward cytotoxic ceramide-inducing drugs.

Inhibition of UGCG induces proapoptotic ceramide/glucosylceramide equilibrium and sensitizes CLL cells to ABT-737-induced apoptosis

Enzymatic activity of UGCG represents a drugable target by specific inhibitors, such as OGB-1 and OGB-2 (UGCGi).[22,23] On average, 74.7% of native primary CLL cells were viable (Figure 4A). The percentage of viable cells was significantly increased after IgM stimulation (84.0%, $P = .0246$) and was not affected after inhibition of UGCG. Because IgM-stimulated CLL cells are known to be more resistant toward chemotherapy compared with unstimulated CLL cells, our next aim was to prove whether inhibition of UGCG might sensitize CLL cells to apoptosis-inducing drugs. Because recently sphingolipids could be identified

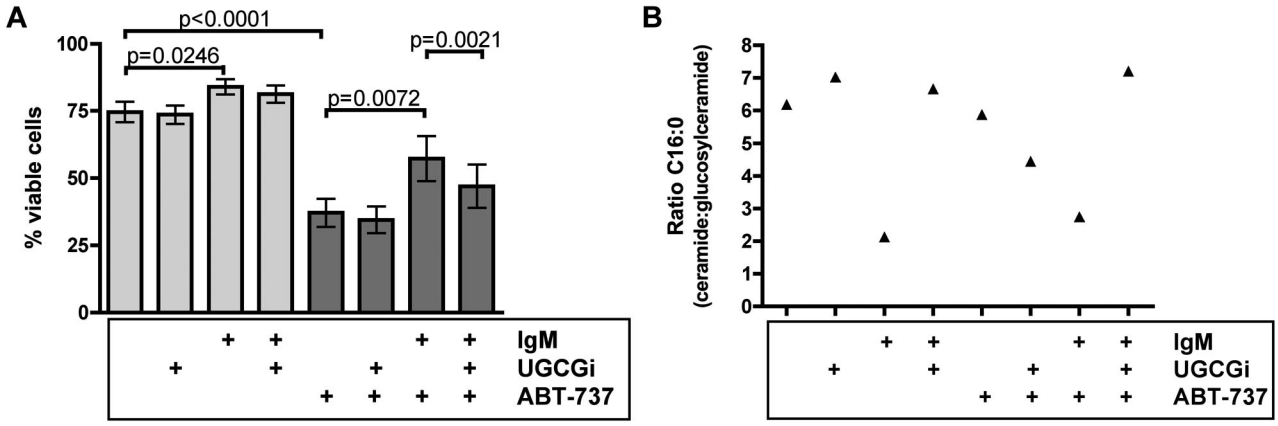

Figure 4. UGCG inhibition sensitizes CLL cells to ABT-737–induced apoptosis. (A) Annexin V/7-amino-actinomycin D staining with subsequent flow cytometry (n = 9). ABT-737 significantly induced apoptosis in CLL cells ($P < .0001$). Whereas IgM stimulation protected CLL cells partly from ABT-737-induced apoptosis ($P = .0072$), UGCG inhibition reverted this effect with a significantly higher amount of apoptotic cells ($P = .0021$). Data are mean ± SEM of 9 independent experiments. Statistics are calculated by paired *t* test. (B) Ceramide/glucosylceramide ratio based on mass spectrometric data exemplarily for fatty acyl chain C16:0 (n = 4). Whereas IgM stimulation led to a lower and thereby glucosylceramide-dominated ratio, inhibition of UGCG reverted the ratio toward ceramide with a concomitant higher quotient after BCR engagement. Protection from ABT-737-induced apoptosis by IgM stimulation was measurable by a glucosylceramide-dominated ratio. UGCG inhibition during ABT-737 treatment and BCR cross-linking resulted in a higher apoptosis rate accompanied by a ceramide-influenced ratio.

as crucial mediators of mitochondria-mediated apoptosis,[24] we have chosen ABT-737 as direct mitochondria-targeting drug. Specifically, there are correlations between BAX/BAK activation via ceramides[24-26]; and above all, promising clinical data have been recently published concerning the BH3 mimetic ABT-263 in treatment of relapsed and refractory CLL.[27] For this reason, we first tested low-dosed ABT-737 (4nM) in primary CLL cells. ABT-737 significantly decreased viability of CLL cells compared with untreated cells (74.7% to 37.2%, $P < .0001$). Supporting our hypothesis, IgM stimulation significantly protected CLL cells from ABT-737-induced apoptosis with 57.3% viable cells ($P = .0072$). Most importantly, we were interested whether decrease of glucosylceramide after IgM stimulation might result in enhanced apoptosis. Therefore, we subsequently inhibited glucosylation of ceramides by inhibition of UGCG with concomitant IgM and ABT-737 treatment. Indeed, we could detect a significant decrease of viable cells (57.3%-47.1%, $P = .0021$). Whereas IgM treatment significantly enhanced cell viability, inhibition of UGCG combined with ABT-737 was able to revert this effect (Figure 4A). However, we wanted to validate our assumption based on our flow cytometry data and investigated whether the influence of the ceramide/glucosylceramide ratio on drug sensitivity was further reflected in mass spectrometric analysis of treated CLL cells (n = 4). Hence, samples corresponding to aforementioned cytotoxicity assays were analyzed as listed: native, native plus UGCG inhibition, IgM-stimulated, and IgM-stimulated plus UGCG inhibition with and without ABT-737 treatment (Figure 4B). Focusing at fatty acyl chain C16:0, which harbors the highest sphingolipid expression of acyl chains, inhibition of UGCG in BCR-untreated CLL cells did not change the ceramide/glucosylceramide ratio. Our previous experiments already identified UGCG to be responsible to shift the ratio toward glucosylceramides after IgM stimulation. IgM treatment reverted the ratio between ceramides and glucosylceramides toward glucosylceramides with and without ABT-737. Most importantly, UGCG inhibition, concomitant with IgM stimulation and ABT-737 treatment, resulted not only in significantly decreased viability of CLL cells but also showed a distinct shift toward a ceramide-dominated ratio (Figure 4B). This indicates that the ceramide/glucosylceramide ratio is a key molecular switch for sensitivity of CLL cells toward induction of apoptosis.

Novel kinase inhibitors sensitize CLL cells toward ABT-737 via UGCG inhibition

After having identified UGCG as relevant enzyme that mediates IgM-induced apoptosis resistance and because IgM is established as driving force of CLL progression in vivo, we were eager to find out whether UGCG is drugable by applying novel kinase inhibitors, which are known to interrupt BCR signaling. Because promising data were recently published concerning the apoptotic influence of the PI3Kδ inhibitor CAL-101 and the BTK inhibitor PCI-32765 in treatment of lymphoid malignancies, including CLL,[6,28-30] we applied both substances to native and IgM-stimulated CLL cells to evaluate their influence on UGCG as a drugable target (n = 9). Indeed, quantitative RT-PCR revealed a significant reduction of UGCG expression after treatment with CAL-101 and PCI-32765 in BCR-stimulated samples ($P = .0039$ for CAL-101, $P = .0078$ for PCI-32765; Figure 5A-B). We further analyzed the influence of both inhibitors on cell viability of primary CLL cells. Our flow cytometric analysis confirmed again a significant increase of cell viability after BCR cross-linking compared with native controls (71.8%-82.9% viable cells, $P = .001$). Treatment with CAL-101 and PCI-32765 resulted in comparable survival rates as native untreated CLL cells (ie, 72.3% for CAL-101 and 74.1% for PCI-32765, respectively), indicating that the chosen drug concentration itself showed only a slight toxicity as a single agent (Figure 5C-D; supplemental Figure 5). Whereas incubation with ABT-737 caused a significant decline of viable CLL cells to 51.3% ($P < .0001$), inhibition of PI3Kδ via CAL-101 and coincubation with ABT-737 significantly intensified this effect with an even synergistic apoptosis rate and only 30.8% viable cells ($P < .0001$). The same could be observed in samples treated simultaneously with ABT-737 and the BTK inhibitor PCI-32765 with a synergistic decline in viability (33.7%, $P = .0004$; Figure 5C-D). Importantly, similar coculture experiments on CD40L-expressing feeder cells resulted in additional but not in a synergistic decline in viability of cells. These data clearly illustrate the effect of tyrosine kinase inhibitors on UGCG expression and thereby on the amount of glucosylceramide, which is not altered by CD40L (supplemental Figure 6). Our results create a rationale to combine ABT-737 with CAL-101 and PCI-32765 (Figure 6).

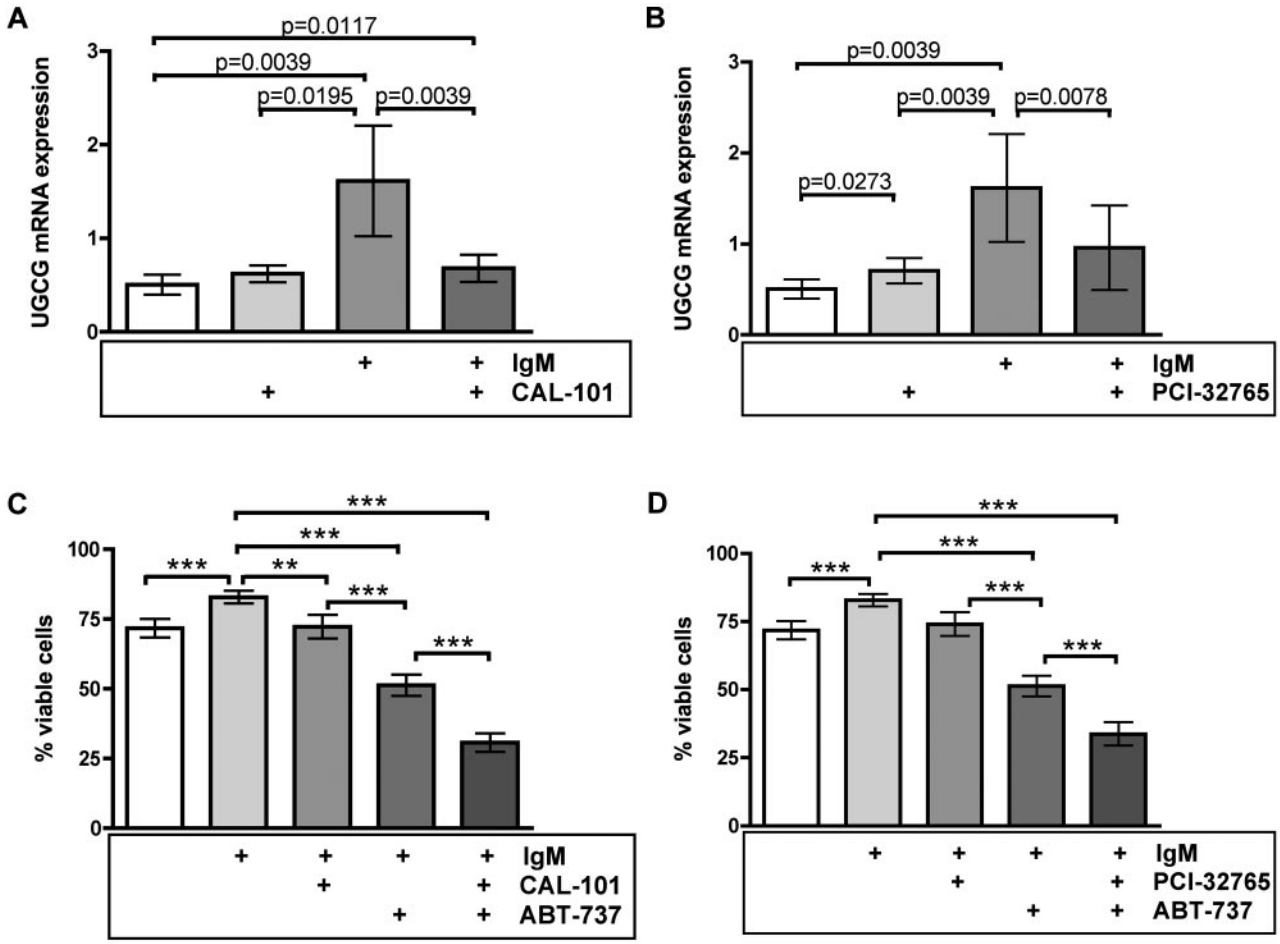

Figure 5. Novel kinase inhibitors sensitize CLL cells toward ABT-737-mediated apoptosis via UGCG inhibition. (A-B) Quantitative RT-PCR was performed for analysis of UGCG expression (n = 9). The PI3Kδ inhibitor CAL-101 as well as the BTK inhibitor PCI-32765 caused a significant reduction of UGCG expression during BCR cross-linking ($P = .0039$ for CAL-101 and $P = .0078$ for PCI-32765). Data are mean ± SEM of 9 independent experiments. Statistics are calculated by Wilcoxon signed-rank test. (C-D) Annexin V/7-amino-actinomycin D staining with subsequent flow cytometry to determine cell viability (n = 15). BCR engagement induced a significant increase of cell survival ($P = .001$), whereas both CAL-101 and PCI-32765 revealed a similar amount of viable CLL cells as native untreated samples. Although ABT-737 led to a significant reduction of cell survival during BCR stimulation ($P < .0001$), the combination of both ABT-737 treatment and concomitant kinase inhibition via CAL-101 or PCI-32765, respectively, caused a significant and presumably synergistic apoptotic effect in IgM-stimulated CLL cells ($P < .0001$ for CAL-101, $P = .0004$ for PCI-32765). Data are mean ± SEM of 15 independent experiments. Statistics are calculated by paired *t* test.

Discussion

Here we investigated the impact of the microenvironment on sphingolipid metabolism-mediated resistance to apoptosis in CLL. We identified sphingolipid metabolism as a novel aspect of BCR-induced apoptosis resistance in primary CLL cells. Our data reveal that balance between proapoptotic ceramide and pro-survival glucosylceramide has an impact on CLL sensitivity toward drugs and is exclusively controlled by BCR but not by CD40L or IL-4. We identified UGCG as the central enzyme, which converts CLL cells toward apoptosis resistance. Although elevated expression level of UGCG could be correlated in prior studies to be associated with drug resistance,[31,32] our data give first functional evidence that UGCG is up-regulated by a pro-survival stimulus. We showed that novel kinase (PI3Kδ and BTK) inhibitors (CAL-101 and PCI-32765) sensitize CLL cells toward cytotoxic drugs by down-regulation of UGCG expression. Interestingly, we were able to identify ABT-737 as a novel compound to apply its cytotoxicity dependent on UGCG expression. Consequently, application of PI3Kδ and BTK inhibitors, with concomitant UGCG repression, and subsequent treatment with ABT-737 resulted in synergistic apoptosis.

Here we report, for the first time, that BCR mediates survival in primary CLL cells via regulation of sphingolipid levels. We could show that BCR-stimulated CLL cells exhibit a significant decreased ceramide level compared with native controls, whereas the amount of pro-survival glucosylceramide was increased. Our analysis illustrates that the ceramide/glucosylceramide ratio became almost completely reverted toward glucosylceramide after IgM stimulation.

It is well known that ceramides are responsible for growth inhibition and apoptosis.[14,15] Nevertheless, it is not fully understood how ceramides are involved in apoptosis. Several mechanisms are described how ceramides contribute to programmed cell death and how they are associated with typical apoptotic characteristics, such as PARP cleavage, DNA fragmentation, or trypan blue uptake.[33] Besides different stimuli, such as certain signaling molecules (protein kinase C or phospholipase A2), death receptors, UV-light, γ-irradiation, or chemotherapy,[34] BCR engagement was shown to play a role in ceramide regulation.[33,35] The Burkitt lymphoma cell line Ramos displayed an increase of C16-ceramide after BCR engagement. In particular, this ceramide species was generated via de novo pathway. In this context, there is evidence

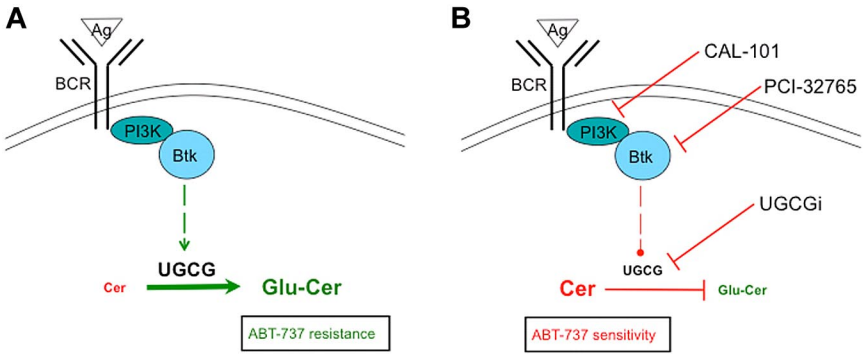

Figure 6. Simplified scheme of BCR-triggered glucosylation of ceramides. (A) BCR engagement results in up-regulation of UGCG expression and glucosylation of ceramides with a concomitant ABT-737 resistance. (B) Direct inhibition of UGCG or repression of UGCG expression via CAL-101 or PCI-32765 after BCR stimulation results in synergistic apoptosis during ABT-737 treatment.

that mitochondrial damage and loss of mitochondrial membrane potential are involved in BCR- and ceramide-mediated apoptosis.[33] This study supports our hypothesis because ceramide up-regulation in Ramos cells results in apoptosis. Our findings also demonstrate a clear down-regulation of C16:0 and C24:1 ceramides but an elevation of glucosylceramides after IgM stimulation of CLL cells. Notably, glucosylceramide concentrations predominated in BCR-engaged samples with a concomitant reversion of the ceramide/glucosylceramide ratio toward glucosylceramide. These findings underline the fact that glucosylceramides contribute to survival and resistance toward apoptosis and chemotherapeutics.[13,31,36] Elevation of glucosylceramide levels was particularly found in resistant cancer cells.[13,31,36-38] This could be proven by the fact that inhibition of glucosylceramide synthesis led to increased sensitization to chemotherapeutics and to cell cycle arrest in different cancer cell lines.[13,39,40]

For instance, competitive enzyme inhibitors, such as PDMP or PPMP, act as structural analogs of the UGCG substrate ceramide with subsequent reduction of glucosylceramide levels.[39,41,42] Further approaches of UGCG inhibition were described,[40,43] including the imino sugars OGB-1 or OGB-2.[22,44] It could be shown that the combination of each imino sugar with specific chemotherapeutics led to a decreased half-maximum inhibitory concentration of drugs, indicating a reduction of drug resistance in CLL samples.[23] We identified UGCG to be responsible for synthesis of glucosylceramide out of ceramide after BCR engagement. Although UGCG seems to be a relevant enzyme that promotes survival in malignant cells, its regulation by physiologic stimuli is completely unknown. Our data give proof, for the first time, that UGCG is up-regulated in established pro-survival settings (eg, BCR engagement), supporting its role as enzyme with antiapoptotic function. Although BCR, CD40L, and IL-4 share some common pathways to promote survival in CLL, our results clearly indicate a substantial difference between those stimuli because BCR exclusively controls UGCG expression and thereby glucosylation of ceramides. Pharmacologic inhibition of this enzyme with concomitant incubation with ABT-737 led to a significantly higher total amount of apoptotic cells. This was confirmed by a reversion of the ceramide/glucosylceramide ratio toward ceramide during IgM stimulation in ABT-737-treated and UGCG-inhibited CLL cells. We assume that ABT-737 leads to increase of apoptotic ceramide, whereas the concomitant blockade of antiapoptotic glucosylceramide synthesis via UGCG inhibition enhances the apoptotic effect. Indeed, there is evidence that ABT-737 is supposed to function via the proapoptotic BAX.[45] BAX activation was shown to be mediated by ceramides/sphingolipids.[25,26] In this context, Chipuk et al showed a clear coordination between sphingolipids and BAX as well as BAK activation during apoptosis.[24]

Recent reports indicate that targeting of the BCR pathway components by the PI3Kδ inhibitor CAL-101 as well as the BTK inhibitor PCI-32765 is promising in CLL.[6,29] Studies verified that CAL-101 exerts its apoptotic effect in primary CLL cells ex vivo but also in first clinical trials.[28,46] Thereby, CAL-101 inhibits BCR-induced survival pathways, including Akt and mitogen-activated protein kinase activation.[6] Concerning PCI-32765, Herman et al could show that inhibition of BTK phosphorylation during BCR cross-linking led to decreased downstream signaling of relevant factors, such as nuclear factor κ B or PI3K.[29] Even pro-survival influences of CLL microenvironment were abrogated by PCI-32765.[29] Clinical activity of this drug is described and will be further analyzed in ongoing studies.[30] Both compounds are known to release CLL cells from the microenvironment into the periphery and are thought to sensitize CLL cells toward apoptosis,[6,47] but their mode of action is mainly unknown. Our data reveal that BCR-mediated apoptosis resistance is disrupted by CAL-101 and PCI-32765 through UGCG repression. Furthermore, promising clinical data of a phase 1 study with ABT-263 have recently been published with clear efficacy in relapsed or refractory CLL patients.[27] Here we identified CAL-101 and PCI-32765 as inhibitors of UGCG expression that are able to sensitize CLL cells toward ABT-737-induced apoptosis, leading to synergistic cell death.

In conclusion, we provide evidence that sphingolipids seems to be critically involved in CLL pathogenesis. Moreover, we identified UGCG as drugable target by novel and specific kinase inhibitors. We showed that controlling the ceramide/glucosylceramide equilibrium results in synergistic apoptotic effects after application of ABT-737. Taken together, the sphingolipid metabolism seems to offer new targets for CLL treatment.

Acknowledgments

J.S., S.B., L.P.F., C.P.P., M.H., and C.-M.W. were supported by the Deutsche Forschungsgemeinschaft (Excellence Cluster 229: Cellular Stress Responses in Aging-Associated Diseases, Bonn, Germany). C.P.P. and C.-M.W. were supported by the German Cancer Aid (DKH109159: Lipid metabolism and signaling as new targets in CLL). C.-M.W. was supported by the CLL Global Research Foundation (Houston, TX).

Authorship

Contribution: L.P.F. and C.-M.W. conceived and designed the present work; J.S., V.F., M.B., M.P., S.B., R.B., J.C., and L.P.F. performed the research; J.S. and L.P.F. conducted statistical

analysis; J.S., C.P.P., M.H., L.P.F., and C.-M.W. analyzed the data; and J.S., L.P.F., C.P.P., and C.-M.W. wrote the manuscript.

Conflict-of-interest disclosure: The authors declare no competing financial interests.

Correspondence: Clemens-Martin Wendtner, University of Cologne, Department I of Internal Medicine, Kerpener Strasse 62, 50937 Cologne, Germany; e-mail: clemens.wendtner@uni-koeln.de.

References

1. Keating MJ, O'Brien S, Albitar M, et al. Early results of a chemoimmunotherapy regimen of fludarabine, cyclophosphamide, and rituximab as initial therapy for chronic lymphocytic leukemia. *J Clin Oncol.* 2005;23(18):4079-4088.
2. Hallek M, Fischer K, Fingerle-Rowson G, et al. Addition of rituximab to fludarabine and cyclophosphamide in patients with chronic lymphocytic leukaemia: a randomised, open-label, phase 3 trial. *Lancet.* 2010;376(9747):1164-1174.
3. Dreger P, Dohner H, Ritgen M, et al. Allogeneic stem cell transplantation provides durable disease control in poor-risk chronic lymphocytic leukemia: long-term clinical and MRD results of the German CLL Study Group CLL3X trial. *Blood.* 2010;116(14):2438-2447.
4. Caligaris-Cappio F. Role of the microenvironment in chronic lymphocytic leukaemia. *Br J Haematol.* 2003;123(3):380-388.
5. Petlickovski A, Laurenti L, Li X, et al. Sustained signaling through the B-cell receptor induces Mcl-1 and promotes survival of chronic lymphocytic leukemia B cells. *Blood.* 2005;105(12):4820-4827.
6. Hoellenriegel J, Meadows SA, Sivina M, et al. The phosphoinositide 3′-kinase delta inhibitor, CAL-101, inhibits B-cell receptor signaling and chemokine networks in chronic lymphocytic leukemia. *Blood.* 2011;118(13):3603-3612.
7. Furman RR, Byrd JC, Brown JR, et al. CAL-101, an isoform-selective inhibitor of phosphatidylinositol 3-kinase P110, demonstrates clinical activity and pharmacodynamic effects in patients with relapsed or refractory chronic lymphocytic leukemia [abstract]. *Blood (ASH Annual Meeting Abstracts).* 2010;116:55.
8. Sharman J, de Vos S, Leonard JP, et al. A phase 1 study of the selective phosphatidylinositol 3-kinase-delta (PI3Kdelta) inhibitor, CAL-101 (GS-1101), in combination with rituximab and/or dendamustine in patients with relapsed or refractory chronic lymphocytic leukemia (CLL) [abstract]. *Blood (ASH Annual Meeting Abstracts.)* 2011;118:1787.
9. Ponader S, Chen SS, Buggy JJ, et al. The Bruton tyrosine kinase inhibitor PCI-32765 thwarts chronic lymphocytic leukemia cell survival and tissue homing in vitro and in vivo. *Blood.* 2012; 119(5):1182-1189.
10. O'Brien S, Burger JA, Blum KA, et al. The Bruton's tyrosine kinase (BTK) inhibitor PCI-32765 induces durable responses in relapsed or refractory (R/R) chronic lymphocytic leukemia/small lymphocytic lymphoma (CLL/SLL): follow-up of a phase Ib/II study [abstract]. *Blood (ASH Annual Meeting Abstracts).* 2011;118:983.
11. Heintel D, Kienle D, Shehata M, et al. High expression of lipoprotein lipase in poor risk B-cell chronic lymphocytic leukemia. *Leukemia.* 2005; 19(7):1216-1223.
12. Pallasch CP, Schwamb J, Konigs S, et al. Targeting lipid metabolism by the lipoprotein lipase inhibitor orlistat results in apoptosis of B-cell chronic lymphocytic leukemia cells. *Leukemia.* 2008;22(3):585-592.
13. Ekiz HA, Baran Y. Therapeutic applications of bioactive sphingolipids in hematological malignancies. *Int J Cancer.* 2010;127(7):1497-1506.
14. Ogretmen B, Hannun YA. Biologically active sphingolipids in cancer pathogenesis and treatment. *Nat Rev Cancer.* 2004;4(8):604-616.
15. Bartke N, Hannun YA. Bioactive sphingolipids: metabolism and function. *J Lipid Res.* 2009; 50(Suppl):S91-S96.
16. Futerman AH, Hannun YA. The complex life of simple sphingolipids. *EMBO Rep.* 2004;5(8):777-782.
17. Pewzner-Jung Y, Ben-Dor S, Futerman AH. When do Lasses (longevity assurance genes) become CerS (ceramide synthases)?: Insights into the regulation of ceramide synthesis. *J Biol Chem.* 2006;281(35):25001-25005.
18. Saddoughi SA, Song P, Ogretmen B. Roles of bioactive sphingolipids in cancer biology and therapeutics. *Subcell Biochem.* 2008;49:413-440.
19. Wendtner CM, Kofler DM, Theiss HD, et al. Efficient gene transfer of CD40 ligand into primary B-CLL cells using recombinant adeno-associated virus (rAAV) vectors. *Blood.* 2002;100(5):1655-1661.
20. Shaner RL, Allegood JC, Park H, et al. Quantitative analysis of sphingolipids for lipidomics using triple quadrupole and quadrupole linear ion trap mass spectrometers. *J Lipid Res.* 2009;50(8): 1692-1707.
21. Signorelli P, Hannun YA. Analysis and quantitation of ceramide. *Methods Enzymol.* 2002;345: 275-294.
22. Andersson U, Butters TD, Dwek RA, Platt FM. N-Butyldeoxygalactonojirimycin: a more selective inhibitor of glycosphingolipid biosynthesis than N-butyldeoxynojirimycin, in vitro and in vivo. *Biochem Pharmacol.* 2000;59(7):821-829.
23. Gerrard G, Butters TD, Ganeshaguru K, Mehta AB. Glucosylceramide synthase inhibitors sensitise CLL cells to cytotoxic agents without reversing P-gp functional activity. *Eur J Pharmacol.* 2009;609(1):34-39.
24. Chipuk JE, McStay GP, Bharti A, et al. Sphingolipid metabolism cooperates with BAK and BAX to promote the mitochondrial pathway of apoptosis. *Cell.* 2012;148(5):988-1000.
25. Kashkar H, Wiegmann K, Yazdanpanah B, Haubert D, Kronke M. Acid sphingomyelinase is indispensable for UV light-induced Bax conformational change at the mitochondrial membrane. *J Biol Chem.* 2005;280(21):20804-20813.
26. Ganesan V, Perera MN, Colombini D, Datskovskiy D, Chadha K, Colombini M. Ceramide and activated Bax act synergistically to permeabilize the mitochondrial outer membrane. *Apoptosis.* 2010;15(5):553-562.
27. Roberts AW, Seymour JF, Brown JR, et al. Substantial susceptibility of chronic lymphocytic leukemia to BCL2 inhibition: results of a phase I study of navitoclax in patients with relapsed or refractory disease. *J Clin Oncol.* 2012;30(5):488-496.
28. Herman SE, Gordon AL, Wagner AJ, et al. Phosphatidylinositol 3-kinase-delta inhibitor CAL-101 shows promising preclinical activity in chronic lymphocytic leukemia by antagonizing intrinsic and extrinsic cellular survival signals. *Blood.* 2010;116(12):2078-2088.
29. Herman SE, Gordon AL, Hertlein E, et al. Bruton tyrosine kinase represents a promising therapeutic target for treatment of chronic lymphocytic leukemia and is effectively targeted by PCI-32765. *Blood.* 2011;117(23):6287-6296.
30. Winer ES, Ingham RR, Castillo JJ. PCI-32765: a novel Bruton's tyrosine kinase inhibitor for the treatment of lymphoid malignancies. *Expert Opin Investig Drugs.* 2012;21(3):355-361.
31. Lavie Y, Cao H, Bursten SL, Giuliano AE, Cabot MC. Accumulation of glucosylceramides in multidrug-resistant cancer cells. *J Biol Chem.* 1996;271(32):19530-19536.
32. Song M, Zang W, Zhang B, Cao J, Yang G. GCS overexpression is associated with multidrug resistance of human HCT-8 colon cancer cells. *J Exp Clin Cancer Res.* 2012;31:23.
33. Kroesen BJ, Pettus B, Luberto C, et al. Induction of apoptosis through B-cell receptor cross-linking occurs via de novo generated C16-ceramide and involves mitochondria. *J Biol Chem.* 2001; 276(17):13606-13614.
34. Carpinteiro A, Dumitru C, Schenck M, Gulbins E. Ceramide-induced cell death in malignant cells. *Cancer Lett.* 2008;264(1):1-10.
35. Kroesen BJ, Jacobs S, Pettus BJ, et al. BcR-induced apoptosis involves differential regulation of C16 and C24-ceramide formation and sphingolipid-dependent activation of the proteasome. *J Biol Chem.* 2003;278(17):14723-14731.
36. Lucci A, Cho WI, Han TY, Giuliano AE, Morton DL, Cabot MC. Glucosylceramide: a marker for multiple-drug resistant cancers. *Anticancer Res.* 1998;18(1B):475-480.
37. Gouaze-Andersson V, Yu JY, Kreitenberg AJ, Bielawska A, Giuliano AE, Cabot MC. Ceramide and glucosylceramide upregulate expression of the multidrug resistance gene MDR1 in cancer cells. *Biochim Biophys Acta.* 2007;1771(12): 1407-1417.
38. Liu YY, Han TY, Giuliano AE, Cabot MC. Ceramide glycosylation potentiates cellular multidrug resistance. *FASEB J.* 2001;15(3):719-730.
39. Rani CS, Abe A, Chang Y, et al. Cell cycle arrest induced by an inhibitor of glucosylceramide synthase: correlation with cyclin-dependent kinases. *J Biol Chem.* 1995;270(6):2859-2867.
40. Liu YY, Han TY, Yu JY, et al. Oligonucleotides blocking glucosylceramide synthase expression selectively reverse drug resistance in cancer cells. *J Lipid Res.* 2004;45(5):933-940.
41. Senchenkov A, Litvak DA, Cabot MC. Targeting ceramide metabolism: a strategy for overcoming drug resistance. *J Natl Cancer Inst.* 2001;93(5): 347-357.
42. Abe A, Inokuchi J, Jimbo M, et al. Improved inhibitors of glucosylceramide synthase. *J Biochem.* 1992; 111(2):191-196.
43. Liu YY, Han TY, Giuliano AE, Hansen N, Cabot MC. Uncoupling ceramide glycosylation by transfection of glucosylceramide synthase antisense reverses adriamycin resistance. *J Biol Chem.* 2000;275(10):7138-7143.
44. Platt FM, Neises GR, Dwek RA, Butters TD. N-Butyldeoxynojirimycin is a novel inhibitor of glycolipid biosynthesis. *J Biol Chem.* 1994;269(11): 8362-8365.
45. Vogler M, Dinsdale D, Sun XM, et al. A novel paradigm for rapid ABT-737-induced apoptosis involving outer mitochondrial membrane rupture in primary leukemia and lymphoma cells. *Cell Death Differ.* 2008;15(5):820-830.
46. Castillo JJ, Furman M, Winer ES. CAL-101: a phosphatidylinositol-3-kinase p110-delta inhibitor for the treatment of lymphoid malignancies. *Expert Opin Investig Drugs.* 2012;21(1):15-22.
47. de Rooij MF, Kuil A, Geest CR, et al. The clinically active BTK inhibitor PCI-32765 targets B-cell receptor- and chemokine-controlled adhesion and migration in chronic lymphocytic leukemia. *Blood.* 2012;119(11):2590-2594.